Stirring-controlled solidified floating solid-liquid drop microextraction as a new solid phase-enhanced liquid-phase microextraction method by exploiting magnetic carbon nanotube-nickel hybrid

Mehri Ghazaghi [a], Hassan Zavvar Mousavi [a, *], Hamid Shirkhanloo [b], Alimorad Rashidi [c]

[a] Department of Chemistry, College of Science, Semnan University, P.O. Box: 35131-19111, Semnan, Iran
[b] Research Institute of Petroleum Industry (RIPI), West Entrance Blvd., Olympic Village, P.O. Box: 14857-33111, Tehran, Iran
[c] Nanotechnology Research Center, Research Institute of Petroleum Industry (RIPI), West Entrance Blvd., Olympic Village, P.O. Box: 14857-33111, Tehran, Iran

HIGHLIGHTS

- Disperser solvent and centrifugation step were eliminated in the proposed method.
- Magnetic carbon nanotube-nickel hybrid was synthesized by one-step approach of spray pyrolysis.
- Magnetic carbon nanotube as an adsorbent and 1-undecanol as organic solvent were participated in the procedure.
- The solid phase enhance extraction efficiency, and easy collection of dispersed solvent droplets.

GRAPHICAL ABSTRACT
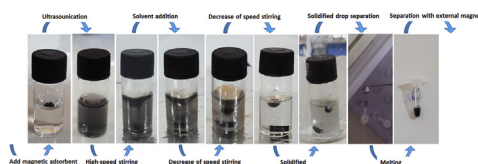
ABSTRACT

A specific technique is introduced to overcome limitations of classical solidification of floating organic drop microextraction, such as tedious and time-consuming centrifuge step and using disperser solvent, by facile and efficient participation of solid and liquid phases. In this proposed method of stirring-controlled solidified floating solid-liquid drop microextraction (SC-SF-SLDME), magnetic carbon nanotube-nickel hybrid (MNi-CNT) as a solid part of the extractors are dispersed ultrasonically in sample solution, and the procedure followed by dispersion of liquid phase (1-undecanol) through high-rate stirring and easily recollection of MNi-CNT in organic solvent droplets through hydrophobic force. With the reduction in speed of stirring, one solid-liquid drop is formed on top of the solution. MNi-CNT acts as both extractor and the coalescence helper between organic droplets for a facile recollection. MNi-CNT was prepared by spray pyrolysis of nickel oleate/toluene mixture at 1000 °C. Four tyrosine kinase inhibitors were selected as model analytes and the effecting parameters were investigated. The results confirmed that magnetic nanoadsorbent has an important role in the procedure and complete collection of dispersed solvent is not achieved in the absence of the solid phase. Also, short extraction time exhibited success of the proposed method and effect of dispersed solid/liquid phases. The limits of quantification (LOQs) for imatinib, sunitinib, erlotinib, and nilotinib were determined to be as low as 0.7, 1.7, 0.6, and 1.0 µg L^{-1}, respectively. The intra-day precisions (RSDs) were lower than 4.5%. Method

---

* Corresponding author.
  E-mail address: hzmousavi@semnan.ac.ir (H.Z. Mousavi).

performance was investigated by determination of mentioned tyrosine kinase inhibitors (TKIs) in human serum and cerebrospinal fluid samples with good recoveries in the range of 93–98%.

1. Introduction

Simple and miniaturized sample treatment by reducing organic solvent or solid phase to donor phase ratio has been tried by microextraction approaches of drop-to-drop technique [1], single drop microextraction (SDME) [2,3], solid-phase microextraction (SPME) [4,5], dispersive liquid–liquid microextraction (DLLME) [6,7], solidified floating organic drop microextraction (SFODME) [8], and dispersive micro solid phase extraction (DμSPE) [9]; each of which has a special property (useful for a specific application) [10]. Among all the available approaches, rapid and efficient techniques are based on dispersion of extraction phase (sorbent or solvent) in sample solution by dispersive force [11]. Effective dispersion of the extractor phase into the sample solution facilitates the process as it maximizes the contact surface between the extractant and the sample and also enhances the mass transfer and the extraction kinetics [12]. Dispersion of liquid extractor can be accomplished by a chemical solvent or via physical force such as, mechanical stirring [13], ultrasound [14], and heating [15]. Chemical dispersion usually participates in the partition distribution of the analytes so that it increases solubility of the analytes in the aqueous phase and reduces the potential efficacy of the method.

Recently introduced solidified floating organic drop microextraction (SFODME) by Zanjani et al. addresses the difficulties in collection of the small microdrops by solidification of extraction solvent [16], and also has several advantages such as low consumption of organic solvent, achievement of high enrichment factor, and compatibility with reversed-phase chromatography [17,18]. Different approaches have been employed to increase the mass transfer rate in the SFODME procedure, including using disperser solvent (DLLME-SFO) [19], ultrasound energy (USAE-SFODME) [20], vortex mixing (VA-SFODME) [21], manual shaking [22], or using surfactants (SA-SFODME) [23]. Ultrasound-assisted solidified floating organic drop microextraction (US-SFODME) has been introduced to overcome the mentioned limitation by applying ultrasound wave as a dispersion force [24]. However, after applying these methods centrifugation step is mandatory to collect extraction phase that prolongs the overall extraction procedure duration and impeding its automation [25].

Introducing magnetic nanoparticles, with exclusive properties, in liquid phase microextraction (LPME) modes can solve such problems [26]. After the classical LPME procedure, a magnetic nanoadsorbent can be utilized to collect solid and liquid phases by an external magnetic force [27]. In contrast to the present research, magnetic nanoadsorbents have been only used for easy separation of extraction solvent without centrifugation step.

Cancer treatment is constantly being developed and new drugs with high molecular activity and pharmacodynamics are constantly advancing. For instance, chronic myeloid leukemia, gastrointestinal stromal tumors, advanced renal cell carcinoma, primary brain tumors, and non-small cell lung cancer are being treated by different selective tyrosine kinase inhibitors (TKIs) of imatinib, nilotinib, erlotinib, and sunitinib [28–31]. No therapeutic window has been clearly defined for the imatinib, erlotinib and nilotinib, but sunitinib therapeutic limit is in the range of 20–200 ng mL^{-1} [32,33]. Nevertheless, they suffer from poor pharmacokinetic characteristics as most of these molecules are metabolized by the internal body enzymes and generate inactive metabolites [34]. Extensive bounding (>95%) of TKIs to plasma and tissue proteins is another drawback that highly limits their penetration into the target cells before performing their pharmacological action [35]. In addition, trace amount of TKIs can pass the blood brain barrier (BBB) and enter the central nervous system (CNS). Concentration of TKIs in cerebrospinal fluid (CSF) can be two orders of magnitude lower than its concentration in plasma [36–38]. To determine low concentrations of free TKIs in plasma and CSF as an essential tool for cancer monitoring facilitates investigation of treatment efficacy and drug-related adverse effects [39]. Introducing sensitive, fast, efficient, and economical sample preparation methods are highly demanded in clinical trials [40].

To eradicate the aforementioned list of the remaining challenges in LPME modes, an advanced technique is described in this report as a serviceable sample treatment approach. Stirring-controlled solidified floating solid-liquid drop microextraction (SC-SF-SLDME) firstly makes use of by high speed stirring to disperse the solidified solvent in the sample solution. Simultaneously with stirring, the ultrasonically dispersed nanoadsorbent is collected in solvent drops and then with decreasing stirring rate droplets of solvent are gathered to make a one solid-liquid drop in surface of the sample solution. In order to develop the method, the proposed SC-SF-SLDME procedure was applied for extraction and preconcentration of four tyrosine kinas inhibitors, as model analytes, in human serum and cerebrospinal fluid sample and effecting parameters were investigated.

2. Experimental

2.1. Reagents and materials

Analytical grade of imatinib mesilate, nilotinib, erlotinib and sunitinib maleate were provided friendly by Parsian Pharmaceuticals Company (Tehran, Iran, parsian-pharma. co). HPLC grade acetonitrile, methanol and water were purchased from Ameretat Shimi (Tehran, Iran, http://www.ameretatco.com). Acetic acid (glacial), ammonium hydroxide (25%), ammonium acetate (≥98%), nitric acid (65%), sodium hydroxide (≥99%), sodium chloride (≥99.5%), toluene (≥99.9%), ethanol (≥99.9%) and nickel nitrate (99%) were prepared from Merck (Darmstadt, Germany; http://www.merckgroup.com). 1-dodecanol (98%), 2-dodecanol (99%), 1-undecanol (99%) and oleic acid (≥99%) were purchased from Sigma-Aldrich Chemie GmbH (Steinheim, Germany). Nitrogen as a carrier gas was used with high purity (99.999%). The stock solutions of four TKIs were prepared by dissolving appropriate amount of them in HPLC-grade methanol at 1000 mg L^{-1} and stored in the dark at 4 °C. The working standard solutions were prepared daily by dilution of their stock standard solutions with HPLC-grade water. Drug-free (blank) human serum and cerebrospinal fluid samples from healthy donors were obtained from the Baqiyatallah Hospital (Tehran, Iran) and transferred into polypropylene test tubes before storage at −20 °C until analysis.

2.2. Instrumental and analytical conditions

Separation and determination of four mentioned TKIs were

performed using a Knauer HPLC system (Berlin, Germany) equipped with a K-1001 HPLC pump, D-14163 online degasser, K-1500 solvent organizer, and a K-2600 UV detector. Chromatographic separation was performed at ambient temperature on Inertsil ODS-3 5 μm column 250 mm × 4.6 mm (GL Science; Tokyo, Japan), protected by a Guard column with Inertsustain C18 (4.0 mm × 3.0 mm) cartridge (GL Science; Tokyo, Japan). The pH of solution was measured by a PHS-3BW model pH-meter (Bell, Italy) and dispersion of magnetic nanoadsorbent was performed with the aid of ultrasonic waves by 50/60 KHz ultrasonic water bath (SW3, Switzerland). Centrifugation was performed by a Hettich centrifuge, model EBA20 (Tuttlingen, Germany), with rotor radius of 50 mm. The CNT-Ni hybrid was synthesized by vertical heating system consists of an electric heating furnace temperature control up to 1200 °C, a reaction zone of 120 cm in length, stainless steel reactor (28 mm inner diameter), and sprayer consisted of two concentric tubes nozzle with inner diameter of 0.8 and 1.8 mm. The synthesized nano material was characterized by transmission electron microscopy (TEM) by Zeiss-EM10C - 80 KV and Raman spectroscopy by Senterra LX200, Bruker Optics, Germany, and high-energy laser diodes with excitation wavelength 785 nm. SEM images were obtained by VEGA//TESCAN-high voltage 15 KV, also elemental analysis was performed using energy dispersive X-ray (EDX-attached to SEM). Magnetic properties of the samples were measured by vibrating sample magnetometer (VSM JDM-13, China) with a maximal applied field of 10 KOe.

2.3. Sample preparation

Preparation of serum samples before SC-SF-SLDME method in order to determine total TKIs (bonded and free) was based on protein precipitation with aid of acetonitrile. In this regard, appropriate volume of TKIs standard solutions were spiked to 2.0 mL serum sample and shaken for 15 min, then 3.0 mL acetonitrile was added to the sample and vortex for 60 s. Then, this mixture was centrifuged for 15 min at 2016 × g at room temperature and the supernatant was transferred into a glass tube and evaporated to dryness at 40 °C under nitrogen stream. The residual was dissolved in 2.0 mL deionized water and SC-SF-SLDME method was done on the final solution.

In order to determine free TKIs in the serum sample, after adding TKIs standard solution and shaking for 20 min for allowing to bind to proteins [41], serum sample was placed in centrifuge filter tube and centrifuged for 10 min at 2016 × g. Bonded TKIs remained in upper part and free TKIs passed thought the filter and collected in lower part, so the serum sample collected in lower part was extracted by proposed SC-SF-SLDME method.

Cerebrospinal fluid was applied in proposed method without protein precipitation.

2.4. Chromatography conditions

The optimum elution for separation of four mentioned TKIs on the analytical column was attained by a composition mobile phase of 20 mmol L^{-1} ammonium acetate (pH = 3.45) (A) and acetonitrile (B) in gradient elution at a flow rate of 1.0 mL min^{-1}. The gradient elution program was as follows: 0–11 min, 5%–95% B; 11–16 min, 95% B; 16–21 min, 95%–5% B; and allowed the chromatographic system to reach equilibrium for 5 min before the next injection. The injection volume was 20 μL and TKIs were monitored at 262 nm.

2.5. Synthesis of carbon nanotube-nickel hybrid

The nickel oleate complex was synthesized by mixing oleic acid and nickel nitrate with molar ratio of 2:1 in the presence of sodium hydroxide (mole ratio equal to oleic acid). The resulted mixture was stirred at 50 °C for 30 min. The synthesized green paste was filtered and washed with EtOH and H$_2$O, then was dried under reduced pressure at 70° C for 6 h.

In order to synthesize MNi-CNT hybrid, a homogeneous solution containing nickel oleate and toluene with concentration of 8% (w/v) was firstly prepared for 15 min via ultrasonication. Nickel oleate was used as a source of catalyst and toluene, a proper solvent for nickel oleate, was used as a carbon source. Magnetic nanoadsorbent was prepared utilizing spray pyrolysis method. In this regard, the nickel oleate-toluene mixture was sprayed with a flow rate of 2.0 mL min^{-1} into the reactor at 1000 °C with aid of nitrogen stream. The pristine synthesized materials contain amorphous carbon. In order to eliminate amorphous carbon, the synthesized material was heated at 300 °C for 30 min.

Synthesis procedure of multiwall carbon nanotube was provided in supporting information.

2.6. Stirring-controlled solidified floating solid-liquid drop microextraction procedure

A 2.0 mL of double distilled water containing 40–50 μg L^{-1} four mentioned TKIs or 2.0 mL of prepared serum and CSF samples (according to section 2.3) with adjusted pH to 11.0, was placed in a ~3 mL vial. After addition appropriate amount of NaCl with final concentration 10% w/v, 1.5 mg MNi-CNT hybrid was added and immersed in an ultrasonic water bath for 30 s. After dispersion of magnetic nanoadsorbent, 30 μL 1-undecanol was inserted in the solution and stirred with glass-coated magnet at rate of 600 rpm for 5 min. After this time, the stirrer speed was decreased to 300 rpm to aggregate solvent drops along with penetration of MNi-CNT into organic solvent. After 1 min stirring at low speed, the solid-liquid floating drop was formed on the surface of the solution. To easy and complete separation of drop from sample solution, the vial was transferred to an ice bath and after 2 min, the solidified solid-liquid drop was moved into conical vial where it melted immediately. Separation of solid and liquid was performed easily with the external magnet. Collected and separated organic solvent respectively from solution and adsorbent was about 22 ± 1 μL 1-undecanol, remaining volume up to 30 μL was compensated by eluting of MNi-CNT with appropriate volume of acetonitrile. Then 20 μL of liquid phase without further dilution injected into the HPLC system for separation and determination. The general procedure represented in Fig. 1.

2.7. Dispersive liquid-liquid microextraction based on solidification of floating organic solvent (DLLME-SFO) procedure

The extraction performance of the SC-SF-SLDME technique was compared with dispersive liquid-liquid microextraction based on solidification of floating organic drop (DLLME-SFO) for determination of TKIs. The DLLME-SFO was performed as follows: 2.0 mL sample solution containing four mentioned TKIs after adjusting pH to 11.0 was placed in conical tube. A binary solution containing 700 μL acetone and 30 μL 1-undecanol was rapidly injected into the sample solution. After centrifugation for 6 min at 2016 × g, the tube was transferred into ice bath; the organic solvent was solidified in 5 min. The solidified solvent was transferred to a conical vial, then melted solvent was injected into HPLC.

3. Results and discussion

3.1. Characterization of MNi-CNT

The morphologies and magnetic properties of MNi-CNT were

characterized by TEM, SEM, Raman spectroscopy and VSM analysis. Fig. S2 (Supplementary material) indicates the Raman spectrum of synthesized hybrid. As can be seen, the D-band and the G-band of MNi-CNT hybrid have appeared at 1303 cm^{-1} and 1574 cm^{-1} respectively. The G-band with its position and shape proved that CNT has been synthesized [42]. The G-band corresponds to in-plane vibration of carbon atoms in the graphene wall of CNTs. The D-band mainly comes from the structure faults in the graphene framework, as holes and edges. The appearance and intensity of D-band located at ~1303 cm^{-1} represents the degree of defects or dangling bonds that it can be interpreted as the formation of nanometer scale amorphous carbon in the MWCNTs or creation of defect due to the presence of nickel nanoparticles within the walls of the synthesized structure [43,44].

Fig. 2a illustrates the SEM images of the synthesized MNi-CNT. It can be seen that diameter of carbon nanotube varied in a range of 50–100 nm.

The nature of the MNi-CNT hybrid was further confirmed by EDX analysis (Fig. S3, Supplementary material). The peaks of Ni and C observed in the EDX image confirmed the existence of nickel and CNT. The relative contents of Ni in the synthesized MNi-CNT can be determined by EDX data. The molar ratios of Ni to C was calculated to be 0.017.

Further structural details of the MNi-CNT were investigated by TEM. Fig. 2b shows the TEM images of MNi-CNT. As shown in Fig. 2b, MNi-CNTs have clean and straight tube walls, including nickel nanoparticles. Typical diameter of MNi-CNT is about 80 nm. The inner and outer diameters of the MNi-CNT are in the range of 20–30 and 60–90 nm (approximately), respectively. Size of nickel nanoparticles are about 10 nm. Also, Fig. 2b clearly shows created defects in the wall of MWCNTs due to the presence of nickel nanoparticles that confirm obtained results from D-band in Raman spectra.

The magnetic property of the MNi-CNT was investigated using vibrating sample magnetometer (VSM) in fields of ±10 KOe at room temperature. The MNi-CNT hysteresis loops are presented in Fig. S4 (Supplementary material). The value of the saturation magnetization (MS) was 740 emu g^{-1}. High saturation magnetization of MNi-CNT illustrated that a high weight ratio of Ni nanoparticles was located into CNT.

TEM images indicate that Ni nanoparticles exist inside the wall of MWCNT, so Ni could not participate in extraction procedure. The other transition-metals that catalyze CNT growth and having magnetic properties such as Fe and Co, could be used in the synthesis process. It can be predicted that Fe and Co will not change extraction efficiency, because the metal in the proposed SC-SF-SLDME technique does not play a role in the extraction, except

easy separation by magnetic force.

The batch-to-batch variation of the MNi-CNT was change in Ni nanoparticle size (10–20 nm), CNT diameters (60–100 nm) and distribution of Ni nanoparticles in wall of the CNT.

3.2. Optimization of the SC-SF-SLDME conditions

Both of the synthesized MNi-CNT hybrid and 1-undecanol were applied in the proposed SC-SF-SLDME method as nanoadsorbent and organic solvent, respectively. In order to investigate necessity of the presence of each phase and effect of different parameters on the proposed method, the SC-SF-SLDME procedure was applied for extraction and determination of four TKIs as model analytes. In this regard, 2.0 mL sample solution containing imatinib, sunitinib, erlotinib and nilotinib was used for each investigation steps.

3.2.1. Effect of pH

pH plays key role in extraction of organic compounds with polar function. In this regard, pH effect on performance of the proposed method was investigated in the range of 2–12 and the results were illustrated in Fig. 3a. As could be seen, extraction performance of four TKIs reached better levels at pH of 11. In lower sample pH extraction recoveries decreased. These results can be interpreted by pK$_a$ values of these analytes. The pK$_a$ values of imatinib, sunitinib, erlotinib and nilotinib are 8.07, 8.95, 5.42 and 13.47, respectively. So, in acidic pH, four mentioned drugs are in cationic forms and cannot penetrate into organic solvent or interact with hydrophobic MNi-CNT, so extraction recovery decrease. But, these basic drugs in the solution with pH near or greater than the pK$_a$ values exist as molecular forms and can be extracted by penetrating into organic solvent or interacting with hydrophobic nanoadsorbent. Based on these results, the sample pH of 11 was selected for more experiments. Lower recoveries at pH of 12.0 may be due to increase the solubility of the 1-undecanol in strong basic solution.

3.2.2. Amount of MNi-CNT hybrid

Magnetic nanoadsorbent acts as a solid extraction phase and has the important role of solvent collection in the proposed SC-SF-SLDME procedure, so selected nanoadsorbent should have hydrophobic surface and magnetic properties. In this goal, magnetic carbon nanomaterials are the best choice, and so magnetic carbon nanotube was selected for applying in the proposed method. The analytes adsorbed on the surface of the synthesized MNi-CNT by hydrophobic interaction. In this regard, to investigate necessity of the present and effect of magnetic nanoadsorbent dosage, different amounts of magnetic MNi-CNT hybrid were examined in the range of 0–3 mg. According to the results shown in Fig. 3b, extraction
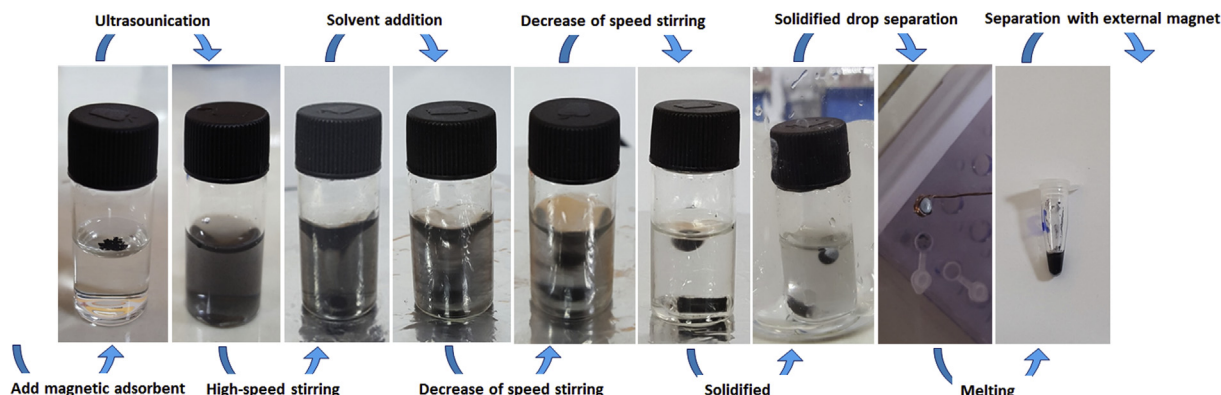

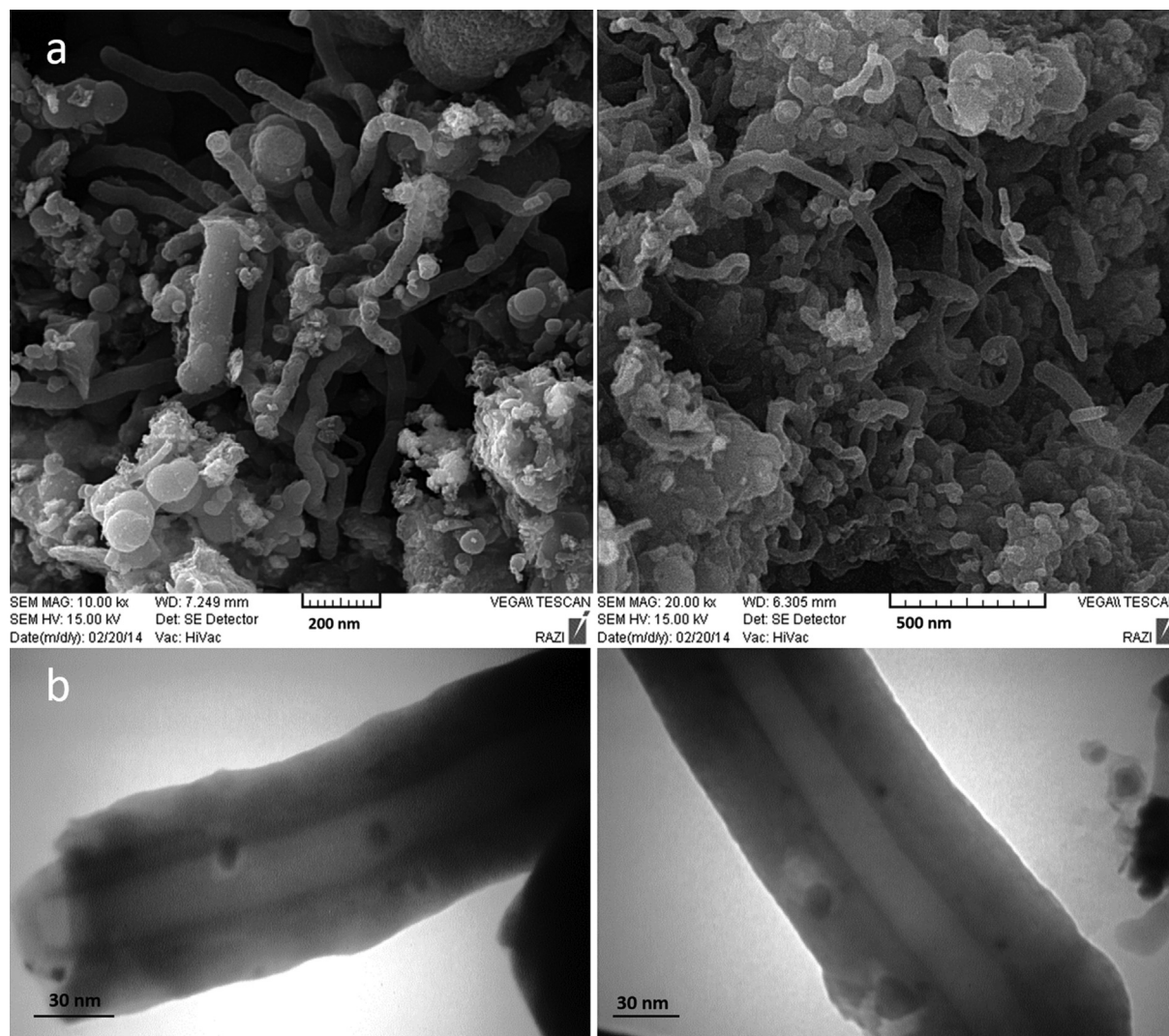**Fig. 1.** Schematic of the proposed SC-SF-SLDME procedure.

Fig. 2. (a) SEM and (b) TEM images of MNi-CNT hybrid.

efficiencies rise with the increase in amount of nanoadsorbent up to 1.5 mg and reach to highest values close to 100% recovery, and further increase lead to reduction of extraction recoveries. In absence of MNi-CNT (zero point in the chart), dispersed organic solvent droplets by high-speed stirring, cannot be aggregated and accumulated completely on the top surface of the solution without centrifugation and the solution remained cloudy. So, very low extraction recoveries were the result of incomplete solvent gathering and absence of auxiliary extraction phase. This result further confirmed the necessity of using nanoadsorbent in the designed SC-SF-SLDME method. On the other hand, larger amount of MNi-CNT (>1.5 mg) not only made the drop heavier, but also nano-adsorbent cannot be completely collected by organic solvent, and the result was a reduction in the extraction recoveries. It should be added that the excess amount of magnetic nanoadsorbent generated the solid-liquid drop with high traction toward a magnet, so the drop was not stable in stirring solution. Therefore, 1.5 mg MNi-CNT hybrid was selected for subsequent studies.

3.2.3. Type and volume of organic solvent

Type of extraction solvent is an important parameter, and this part of the extraction phase should have some characteristics; low toxicity, low volatility, low water solubility, near room temperature melting point (in the range of 10–30 °C), compatible with analytical instrument and good extraction efficiency. So, 1-undecanol, 1-dodecanol and 2-dodecanol were chosen for investigation. The results of this study (Table S1) showed that 1-undecanol, despite higher viscosity, had higher extraction efficiencies. The differences in extraction efficiencies may be due to higher polarity of 1-undecanol in compare to 1-dodecanol and 2-dodecanol. Also, 1-undecanol had better chromatographic behavior and solvent peak was not interfere with analytes' peak, so that several noise appeared before coming out of the first analyte and caused unstable baseline. But, 1-dodecanol and 2-dodecanol had serious interfere. On the other hand, 1-undecanol has lower melting point (16 °C) compare to 1-dodecanol (21–24 °C) and 2-dodecanol (19 °C) which is an advantage when separation was done on column at room temperature. Consequently, 1-undecanol was used in subsequent studies. It should be pointed out that the injection of 1-undecanol to LC is limitation of this method (cause momentary high pressure at time of injection and unstable baseline), but along with more advantages of the method, it is not serious and can be neglected.

In the SC-SF-SLDME approach, organic solvent acts as an extraction phase and solid-phase collector, also after separation from solid part was injected directly to HPLC. So, volume of 1-
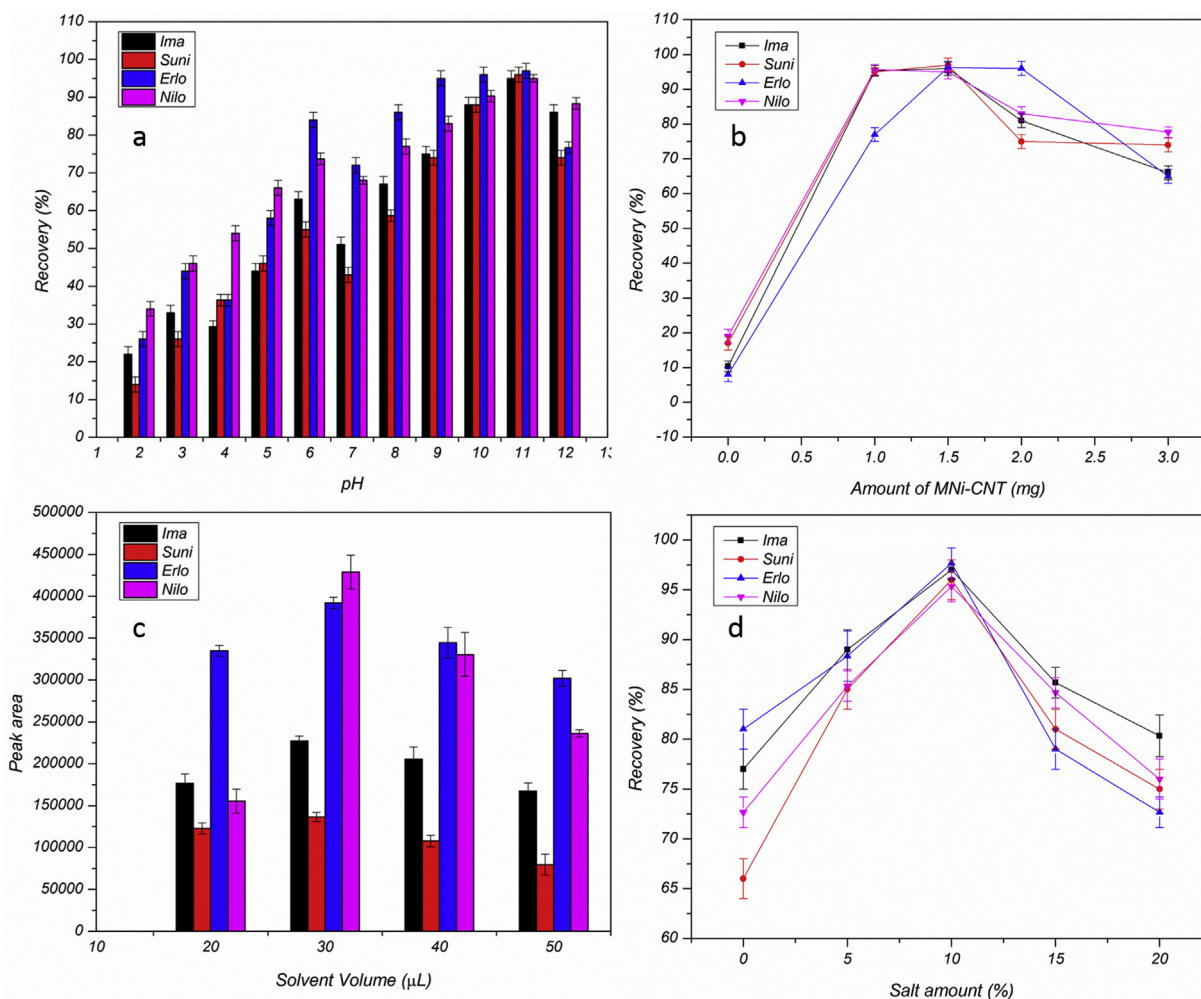
Fig. 3. (a) Effect of sample pH, Conditions: 2.0 mL sample solution containing 50 μg L^{-1} of each TKIs, 30 μL 1-undecanol, 1.5 mg MNi-CNT, 10% NaCl, extraction time: 10 min; (b) Effect of MNi-CNT amount, Conditions: 2.0 mL sample solution (pH 11) containing 50 μg L^{-1} of each TKIs, 30 μL 1-undecanol, 10% NaCl, extraction time: 10 min; (c) Effect of 1-undecanol volume, Conditions: 2.0 mL sample solution (pH 11) containing 50 μg L^{-1} of each TKIs, 1.5 mg MNi-CNT, 10% NaCl, extraction time: 10 min; and (d) Effect of salt amount, Conditions: 2.0 mL sample solution (pH 11) containing 50 μg L^{-1} of each TKIs, 1.5 mg MNi-CNT, 30 μL 1-undecanol, extraction time: 10 min. (Mean of three determinations ± standard deviation).

undecanol is an effective parameter not only in extraction efficiency, but also in the solid phase collection and enrichment factor. In this regard, different volumes of 1-undecanol in the range of 20−50 μL were investigated and the results are presented in Fig. 3c. The lowest volume was limited to the required volume for injection to HPLC for analysis, so 20 μL was selected as lowest volume for investigating. Maximum extraction efficiencies were obtained by 30 μL 1-undecanol and remained constant with further increase. According to the results appropriate volume for quantitative extraction of analytes was 30 μL, and lower volumes were not sufficient for collecting the solid phase and trapping the analytes from solution. Higher volumes lead to unnecessary dilution of analytes.

3.2.4. Salt effect

Commonly, salt addition improves the extraction recoveries of the relatively polar analytes as a result of the salting-out effect. So, the effect of salt addition (NaCl) on extraction recoveries of the four TKIs by the proposed method was investigated over the range of 0−25% and the results are presented in Fig. 3d. Increasing the amount of NaCl from 0 to 10%, increased the extraction recoveries. Salting out phenomenon can interpret this increase in recovery by

decreasing the solubility of the TKIs and improving the analytes transfer to the liquid phase. On the other hand, further increase in concentration of salt reduced the extraction recoveries. This can be explained by the salting in event. At high concentration of NaCl, sample viscosity increases and prevents the transport of the analytes to the extracting solvent, so, the more concentrated of salt, the more difficult diffusion of the analytes. Also, solubility of the 1-undecanol increases with increasing concentration of salt. Therefore, 10% NaCl was chosen for further studies.

3.2.5. Extraction time and temperature

Exposure time guarantees the equilibrium between aqueous and organic phases, so increases the precision and sensitivity. In the SC-SF-SLDME method extraction time was defined as the time of high-speed stirring. To select an optimum exposure time, a series of experiments were designed to investigate the effect of time on extraction recovery over the range of 2−15 min. The results showed that the extraction recoveries increased with the increase of time, and then reached a plateau after 5 min. So, 5 min was chosen as the optimum time for the proposed method. In compare to classical solidified microextraction methods [45,46], the SC-SF-SLDME approach is very fast and this may be due to the participation of

the dispersed MNi-CNT and solvent drops.

Effect of temperature on extraction recoveries was studied in the range of 20–70 °C. The results indicated that the extraction efficiencies did not show a significant change up to 70 °C. This may be due to the participation of the solid phase in extraction procedure. Therefore, extraction at room temperature was selected.

3.2.6. Role of MNi-CNT and Ni in the SC-SF-SLDME method

The responsibility of the magnetic adsorbent in the proposed SC-SF-SLDME approach can be divided in two parts, extraction/adsorption of analytes and implementation of the procedure. In order to unfold role of magnetic nanoadsorbent in adsorption of analytes, magnetic dispersive micro solid phase extraction was performed by applying 1.5 mg the MNi-CNT for 2 mL sample solution at pH 11. Because the MNi-CNT attach to the magnet (inside the solution) at low-speed stirring and in the absence of solvent lighter than water, after sonication for dispersion of magnetic nanoadsorbent, the solution was shaken for 5 min and then separated by external magnet. The obtained recoveries were as follows: 45% ± 1.9, 37% ± 2.1, 55% ± 2.2 and 25% ± 1.8 for imatinib, sunitinib, erlotinib and nilotinib, respectively. These results show that the MNi-CNT alone is not able to extract four TKIs quantitative and these analytes have relatively low affinity toward the hydrophobic surface of the MNi-CNT. However, it is clear that the MNi-CNT contribute in the extraction of analytes. Obtained results from section of 3.2.2 can describe the role of magnetic nanoadsorbent in implementation of the procedure. In the absence of the MNi-CNT, dispersed solvent cannot recollect completely and so recoveries decrease effectively. Strings of CNTs with hydrophobic surface move in sample solution by stirring and dispersed drops of hydrophobic solvent attach to these chains, so even very small drops attach to the MNi-CNT and easily collect. Therefore, the MNi-CNT acts as a junction between solvent drops or as a strong skeleton to aggregate organic droplets. In the absence of the MNi-CNT, drops cannot be separated completely and the solution remained cloudy.

To clarify the importance of Ni in this procedure, MWCNTs (lack of Ni) was applied in the SC-SF-SLDME procedure instead of the MNi-CNT. Because of the lack of magnetism adsorbent, centrifugation was used to separate liquid and solid phases, and also higher volume of liquid phase (40 μL) was applied to provide sufficient volume for injection into HPLC. Significant changes were not shown in extraction efficiencies. Ni nanoparticles play important role in easy solid-liquid separation step and does not play a role in extraction, as previously predicted. Due to complete separation of solid and liquid phases without centrifugation, the low volume of solvent can be used.

Ni was chosen over the other options (Co, Fe) for synthesizing magnetic CNT, due to the weaker magnetic properties [47]. Since the magnetic CNT was applied in solution in the presence of the glass-coated magnet, strong magnetic nanoparticles attaches to the magnet in stirring solution instead of dispersing. So, the use of strong magnetic nanoparticles (Fe-CNT or Co-CNT) is an obstacle to the implementation of the proposed method. The MNi-CNT remain dispersed in stirring sample solution by the magnet.

3.3. Analytical performance

The analytical characteristics of the developed method, such as the limit of detection and quantification, reproducibility, correlation coefficient, linear dynamic ranges (LDRs) and enrichment factors were determined by processing 2.0 mL standard solution of imatinib, sunitinib, erlotinib and nilotinib and the results are summarized in Table 1. The limit of detections were determined as a signal-to-noise ratio of 3 (S/N = 3) by comparing measured signals from samples with known low concentrations of TKIs with those of blank samples, and obtained LODs were as follows: 0.2, 0.5, 0.15 and 0.25 μg L^{-1} for imatinib, sunitinib, erlotinib and nilotinib, respectively. Also, limit of quantifications were determined based on signal-to-noise ratio of 10 (S/N = 10) method, similar to LOD, and obtained LOQs were 0.7, 1.7, 0.6 and 1.0 μg L^{-1} for imatinib, sunitinib, erlotinib and nilotinib, respectively. The corresponding linear dynamic ranges (LDRs) exhibited high-quality linear relationships over the ranges of 0.7–110 μg L^{-1} for imatinib, 1.7–190 μg L^{-1} for sunitinib, 0.6–110 μg L^{-1} for erlotinib and 1.0–190 μg L^{-1} for nilotinib with good correlation coefficients higher than 0.992. To clearly assess sample matrix effects, matrix-match calibrations (standards added to blank serum and CSF samples) were statistically compared with calibration curves from standard solutions. Existence of matrix effect demonstrates in the calibration equations by changes in the slope and intercept of the calibration curves. For this purpose, serum and CSF samples free of TKIs were spiked at different concentration levels. Determination coefficients (R^2) for all the TKIs were obtained higher than 0.99. The F-test was applied to statistically evaluate the slope differences between standard and matrix-matched calibration curves. The results ($F_{2,2} = 0.29$–0.87, P = 0.17–0.73) revealed that slope differences were not considered statistically significant and so considerable matrix effects did not occur. So, results show that the two different types of calibration curve, in water and matrix-match calibration, are identical and calibration curves in water can be used for TKIs quantification without the need for any matrix-match calibration. The repeatability of the presented method was estimated by ten replicated extractions of four TKIs at three concentrations of LOQs, 50 and 100 μg L^{-1}, so intraday relative standard deviations (RSDs) were obtained in the range of 3.6–4.5 for middle concentration level of 50 μg L^{-1}. As well as, the reproducibility of the method, inter-day RSDs of five replicates in five different days were measured and results indicated in Table 1. The specificity of the proposed extraction method was tested using 6 different blank human serum samples spiked at 50 μg L^{-1} of each TKIs and the results indicated absence of any interfering peaks at the TKIs retention times and acceptable RSDs in the range of 4.2–4.9% that confirmed specificity of the method. Characterization factors for preconcentration method such as enrichment factor (EF) and consumptive index (CI) were also determined. Enrichment factor was calculated as the slope ratio of the calibration graph of the SC-SF-SLDME procedure to that of the calibration graph without preconcentration and the consumptive index (CI) was defined as the sample volume (mL) consumed to reach a unit of enrichment factor (EF), and calculated by the ratio between the volume of the sample (mL) and EF (CI =Vs (mL)/EF, where Vs is the sample volume). Obviously, the enrichment factor is considered in conjunction with the sample volume and CI is a better index for describing preconcentration procedure. The lowest consumptive index was achieved by consuming lowest sample volume to obtain highest enrichment factor. Low CI amounts obtained for the SC-SF-SLDME method, confirm capability of this technique to achieve high EF by using low sample volume.

3.4. Application of SC-SF-SLDME method to biological samples

In order to investigate the matrix effect and accuracy of the proposed method, the developed SC-SF-SLDME approach was applied to the simultaneous analysis of four TKIs in human serum and cerebrospinal fluid samples. Human real samples were spiked with the four TKIs standard solutions at different concentrations in corresponding linear ranges. As previously mentioned, protein binding of TKIs are more than 95%, so determination of free and total the TKIs in serum samples were performed in a separate sample preparation procedure presented in section of 2.3, then the

Table 1
Analytical performance of the SC-SF-SLDME technique (mean ± SD, n = 3).

Parameter	Imatinib	Sunitinib	Erlotinib	Nilotinib
Enrichment factor	255	134	575	160
Consumptive index (mL)	0.008	0.015	0.003	0.012
Detection limit ($\mu g\ L^{-1}$; n = 10)	0.2	0.5	0.15	0.25
Limit of quantification ($\mu g\ L^{-1}$; n = 10)	0.7	1.7	0.6	1.0
Intra-day precision (RSD %, n = 10)	7.1 (0.7 $\mu g\ L^{-1}$)[a]	7.7 (1.7 $\mu g\ L^{-1}$)	6.8 (0.6 $\mu g\ L^{-1}$)	7.3 (1.0 $\mu g\ L^{-1}$)
	4.0 (50 $\mu g\ L^{-1}$)[b]	4.5 (50 $\mu g\ L^{-1}$)	3.6 (50 $\mu g\ L^{-1}$)	4.3 (50 $\mu g\ L^{-1}$)
	3.1 (100 $\mu g\ L^{-1}$)[c]	3.7 (100 $\mu g\ L^{-1}$)	2.9 (100 $\mu g\ L^{-1}$)	3.2 (100 $\mu g\ L^{-1}$)
Inter-day precision (RSD %, n = 5)	12.1 (0.7 $\mu g\ L^{-1}$)	12.7 (1.7 $\mu g\ L^{-1}$)	9.8 (0.6 $\mu g\ L^{-1}$)	13.4 (1.0 $\mu g\ L^{-1}$)
	7.0 (50 $\mu g\ L^{-1}$)	7.5 (50 $\mu g\ L^{-1}$)	6.3 (50 $\mu g\ L^{-1}$)	7.2 (50 $\mu g\ L^{-1}$)
	5.9 (100 $\mu g\ L^{-1}$)	6.3 (100 $\mu g\ L^{-1}$)	5.1 (100 $\mu g\ L^{-1}$)	6.5 (100 $\mu g\ L^{-1}$)
Linear range ($\mu g\ L^{-1}$)	0.70–110	1.70–190	0.60–110	1.0–190
Correlation coefficient	0.996	0.995	0.999	0.992
Regression equation ($\mu g\ L^{-1}$) $Y = (a \pm SD_a)X + (b \pm SD_b)$	y = (23,340.153 ± 102) [ima]–(121.94 ± 8.4)	y = (4121.00 ± 98.3) [suni]–(317.29 ± 21.3)	y = (45,873.269 ± 865) [erlo] + (118.04 ± 9.6)	y = (25,229.678 ± 689) [nilo]–(169.43 ± 11.4)

SD_a, SD_b: standard deviation of slop and intercept, respectively.
[a] Precision at 2 $\mu g\ L^{-1}$.
[b] Precision at 50 $\mu g\ L^{-1}$.
[c] Precision at 100 $\mu g\ L^{-1}$.

SC-SF-SLDME method was applied (n = 3) for extraction and pre-concentration of mentioned TKIs from serum samples. The results were listed in Table 2. The recoveries in the range of 85–99% exhibited that the present method was effective and reliable for the determination of TKIs in complex matrixes. The typical chromatograms of non-spiked and spiked human serum and CSF with four TKIs are presented in Fig. 4. The chromatograms of non-spiked and spiked human serum with 2.0 $\mu g\ L^{-1}$ of four TKIs is presented in Fig. 4a. Also, chromatogram of spiked serum sample at 2.0 $\mu g\ L^{-1}$ of four TKIs, prepared with protein precipitation and without preconcentration, was presented in Fig. 4a for comparing. Fig. 4b presents the chromatograms of non-spiked and spiked human serum with 30.0 $\mu g\ L^{-1}$ of four TKIs. The chromatograms of non-spiked and spiked human CSF sample with 40.0 $\mu g\ L^{-1}$ of four TKIs is presented in Fig. 4c.

A comparison of the proposed method with the only reported method for determination of imatinib, sunitinib, erlotinib and nilotinib can be found in Table 3. As can be seen, the presented method possesses a wide range of linearity, low detection limit, high sensitivity, and low consumption of sample volume for simultaneous extraction of the TKIs. LODs of the SC-SF-SLDME method were comparable with the reported method only with the use of 2.0 mL sample solution. Also, higher enrichment factors obtained with preconcentration of lower sample volume while having better precision indicate that the presented method is applicable and reliable for detection of the TKIs. Also in comparing with other reported method, the SC-SF-SLDME procedure is fast and easy to do.

To demonstrate the advantages and the ability of the proposed approach in solving problems of existing methods, extraction performance of the SC-SF-SLDME technique was compared with dispersive liquid-liquid microextraction based on solidification of floating organic drop (DLLME-SFO) in the determination of TKIs. Extraction efficiencies of imatinib, sunitinib, erlotinib and nilotinib by the SC-SF-SLDME approach were 95 ± 3.8, 93 ± 4.1, 94 ± 4.4 and 97 ± 3.5, respectively. Whereas, Extraction efficiencies by the DLLME-SFO method were obtained as 60 ± 2.5, 42 ± 2.1, 63 ± 1.9 and 55 ± 2.3 for imatinib, sunitinib, erlotinib and nilotinib, respectively. Lower extraction recoveries by using the DLLME-SFO method may be due to using disperser solvent that cause

Table 2
Determination of free and whole TKIs in human serum and whole TKIs in cerebrospinal fluid samples by proposed SC-SF-SLDME method under optimum conditions (mean ± SD, n = 3).

Sample	Added ($\mu g\ L^{-1}$)				Found[a] ($\mu g\ L^{-1}$)				Recovery (%)			
	Ima	Suni	Erlo	Nilo	Ima	Suni	Erlo	Nilo	Ima	Suni	Erlo	Nilo
Human Serum	–	–	–	–	ND[b]	ND	ND	ND	–	–	–	–
	0.7	1.7	0.6	1.0	0.6 ± 0.05	1.5 ± 0.1	0.52 ± 0.04	0.84 ± 0.07	85.7	88.2	86.7	84.0
	50	50	50	50	46.7 ± 2.3	46.8 ± 2.1	47.8 ± 2.2	48.4 ± 2.9	93.4	93.6	95.6	96.8
	100	100	100	100	94.4 ± 4.0	96.7 ± 4.4	97.3 ± 3.8	94.5 ± 4.1	94.4	96.7	97.3	94.5
	–	150	–	150	–	142.4 ± 5.7	–	143.5 ± 5.8	–	94.9	–	95.6
Human CSF	–	–	–	–	ND	ND	ND	ND	–	–	–	–
	0.7	1.7	0.6	1.0	0.65 ± 0.05	1.56 ± 0.1	0.54 ± 0.04	0.95 ± 0.08	92.8	91.8	90.0	95.0
	50	50	50	50	47.9 ± 2.2	47.8 ± 3.1	48.8 ± 2.5	48.9 ± 2.9	95.8	95.6	97.6	97.8
	100	100	100	100	97.6 ± 3.4	97.7 ± 4.0	98.5 ± 4.2	98.5 ± 3.9	97.6	97.7	98.5	98 0.5
	–	150	–	150	–	143.8 ± 5.3	–	144.1 ± 5.7	–	95.9	–	96.1

					Found[a] ($\mu g\ L^{-1}$)				Protein binding (%)			
					Free Ima	Free Suni	Free Erlo	Free Nilo	Ima	Suni	Erlo	Nilo
Human Serum[c]	50	100	50	100	2.9 ± 0.2	4.6 ± 0.3	1.5 ± 0.1	1.4 ± 0.2	94.2	95.4	97	98.6
	100	150	100	150	4.8 ± 0.4	6.7 ± 0.4	3.7 ± 0.3	2.3 ± 0.3	95.2	95.4	96.3	98.5

[a] Mean value ± standard deviation based on three replicate measurements.
[b] Not detected.
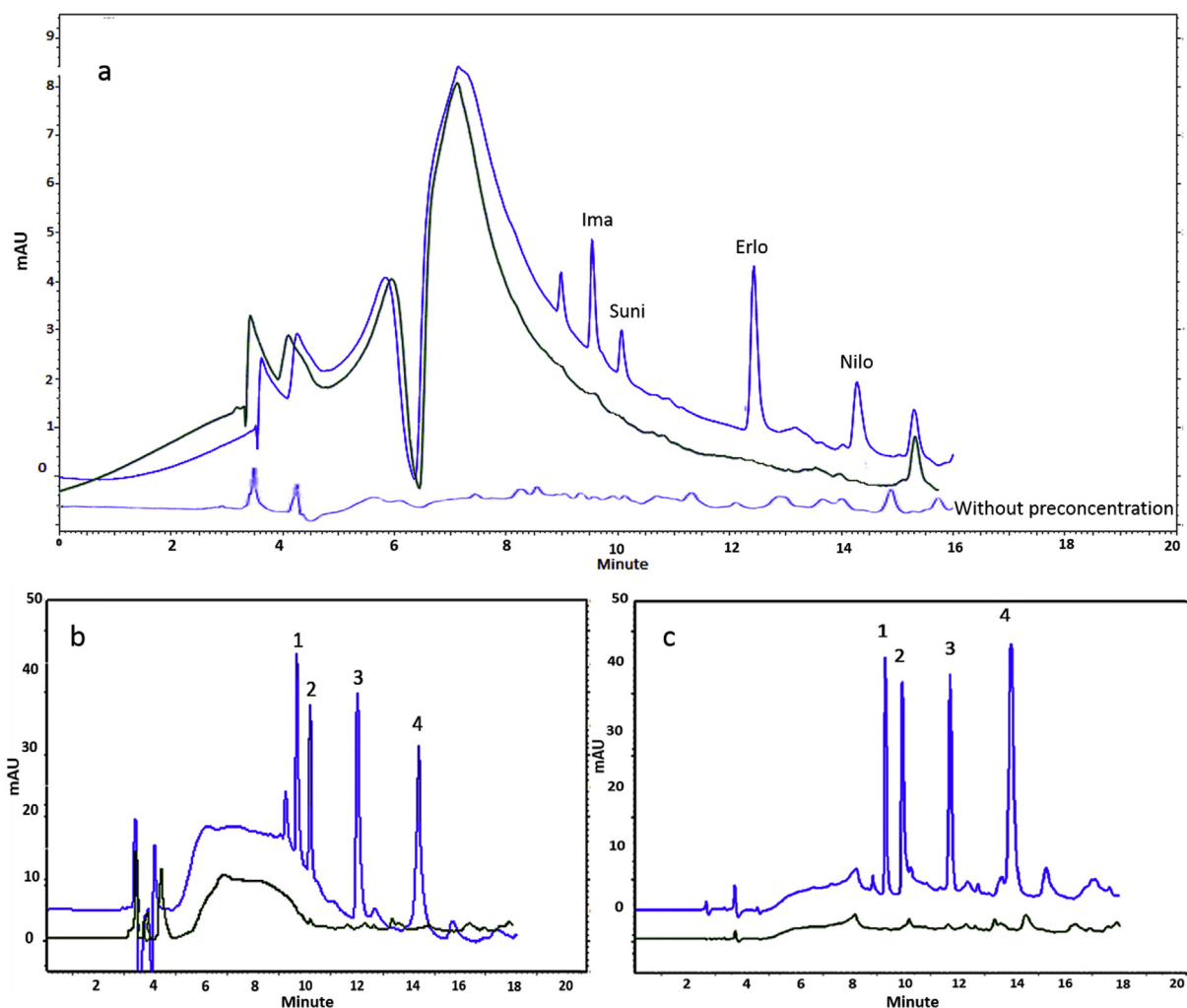[c] Prepared for determination of free TKIs.

Fig. 4. Representative chromatograms under optimal SC-SF-SLDME conditions. Human serum sample, green line: non-spiked serum sample, blue line: spiked serum sample (a) at 2 µg L^{-1} of each TKIs and (b) at 30 µg L^{-1} of each TKIs. (c) Human CSF sample, green line: non-spiked CSF sample, blue line: spiked CSF sample at 40 µg L^{-1} of each TKIs. (1) Imatinib, (2) Sunitinib, (3) Erlotinib, (4) Nilotinib. (For interpretation of the references to colour in this figure legend, the reader is referred to the web version of this article.)

increase analytes and solvent solubility in solution and decrease partition coefficient. The good performance of the proposed method was probably due to several reasons such as the use of high-speed stirring instead of disperser solvent for dispersion of extraction solvent, participation of the solid phase in extraction procedure, and also the complete separation of extraction solvent from sample by solid phase through hydrophobic force. This procedure utilizes two dispersed extraction phases (solid and liquid).

Moreover, centrifugation step, obstacle for automation, had been removed.

4. Conclusions

The simple and reliable method was presented to address disadvantages of single drop microextraction and dispersive mode of liquid phase microextraction (LPME). Magnetic carbon nanotube-

Table 3
Comparison of the SC-SF-SLDME procedure with published method for preconcentration and extraction of TKIs.

TKIs	Method	Detection	Matrix	LOD (µg L^{-1})	RSD %	Calibration range (µg L^{-1})	PF/EF	Sample volume	Ref.
Imatinib, Sunitinib, Erlotinib, Nilotinib, Axitinib, Gefitinib, Dasatinib	solid-phase extraction	UPLC/ MS-MS	Plasma	1.1 dasatinib and axitinib 0.4 gefitinib and sunitinib	13.1 and 14.2%	0.1/0.4–200	30[b]	5.0 mL	[48]
Imatinib, Sunitinib, Erlotinib, Nilotinib	SC-SF-SLDME	HPLC -UV	Serum and CSF	0.18, 0.46, 0.13, 0.23	4.2, 4.5, 3.9 and 4.4%	0.60–110, 1.6–190, 0.51–110, 0.8–190	255, 134, 575 and 160[a] 66.6[b]	2.0 mL	This study

[a] Slopes ratio of calibration curves of analyte after preconcentration to that prior preconcentration (PF).
[b] Volume ratio before and after preconcentration (EF).

nickel hybrid as a solid phase extractor/solvent collector and 1-undecanol as liquid phase extractor/solid phase collector were used in this method. These two phases complement each other in running this method and dispersed solvent with high-speed stirring could not be completely recollected in the absence of adsorbent. The proposed SC-SF-SLDME method was developed for extraction of imatinib, sunitinib, erlotinib and nilotinib from biological samples. Reduced extraction time in comparison to the classical method clearly showed the success of the partnership of dispersed nanoadsorbent and dispersed organic solvent in extraction procedure. Also The SC-SF-SLDME method can be automated. This research proves that by applying solid phase can solve the obstacles of liquid phase microextraction methods so bright future is expected for extraction methods.

Acknowledgments

Appendix A. Supplementary data

Supplementary data related to this article can be found at http://dx.doi.org/10.1016/j.aca.2016.11.034.

References

[1] H. Liu, P.K. Dasgupta, Analytical chemistry in a drop. Solvent extraction in a microdrop, Anal. Chem. 68 (1996) 1817–1821.
[2] M.A. Jeannot, F.F. Cantwell, Solvent microextraction into a single drop, Anal. Chem. 68 (1996) 2236–2240.
[3] L. Li, B. Hu, L. Xia, Z. Jiang, Determination of trace Cd and Pb in environmental and biological samples by ETV-ICP-MS after single-drop microextraction, Talanta 70 (2006) 468–473.
[4] C. Dietz, J. Sanz, C. Cámara, Recent developments in solid-phase microextraction coatings and related techniques, J. Chromatogr. A 1103 (2006) 183–192.
[5] A.K. Malik, V. Kaur, N. Verma, A review on solid phase microextraction—high performance liquid chromatography as a novel tool for the analysis of toxic metal ions, Talanta 68 (2006) 842–849.
[6] M. Rezaee, Y. Assadi, M.-R.M. Hosseini, E. Aghaee, F. Ahmadi, S. Berijani, Determination of organic compounds in water using dispersive liquid–liquid microextraction, J. Chromatogr. A 1116 (2006) 1–9.
[7] S. Berijani, Y. Assadi, M. Anbia, M.-R.M. Hosseini, E. Aghaee, Dispersive liquid–liquid microextraction combined with gas chromatography-flame photometric detection: very simple, rapid and sensitive method for the determination of organophosphorus pesticides in water, J. Chromatogr. A 1123 (2006) 1–9.
[8] S. Dadfarnia, A.M. Salmanzadeh, A.M.H. Shabani, A novel separation/preconcentration system based on solidification of floating organic drop microextraction for determination of lead by graphite furnace atomic absorption spectrometry, Anal. Chim. Acta 623 (2008) 163–167.
[9] W.-H. Tsai, H.-Y. Chuang, H.-H. Chen, J.-J. Huang, H.-C. Chen, S.-H. Cheng, T.-C. Huang, Application of dispersive liquid–liquid microextraction and dispersive micro-solid-phase extraction for the determination of quinolones in swine muscle by high-performance liquid chromatography with diode-array detection, Anal. Chim. Acta 656 (2009) 56–62.
[10] G. Lasarte-Aragonés, R. Lucena, S. Cárdenas, M. Valcárcel, Effervescence assisted dispersive liquid–liquid microextraction with extractant removal by magnetic nanoparticles, Anal. Chim. Acta 807 (2014) 61–66.
[11] M. Cruz-Vera, R. Lucena, S. Cárdenas, M. Valcárcel, Sample treatments based on dispersive (micro) extraction, Anal. Method 3 (2011) 1719–1728.
[12] E. Psillakis, N. Kalogerakis, Developments in single-drop microextraction, TrAC Trends Anal. Chem. 21 (2002) 54–64.
[13] X.-M. Sun, Y. Sun, L.-W. Wu, C.-Z. Jiang, X. Yu, Y. Gao, L.-Y. Wang, D.-Q. Song, Development of a vortex-assisted ionic liquid microextraction method for the determination of aromatic amines in environmental water samples, Anal. Method 4 (2012) 2074–2080.
[14] Q. Zhou, X. Zhang, J. Xiao, Ultrasound-assisted ionic liquid dispersive liquid-phase micro-extraction: a novel approach for the sensitive determination of aromatic amines in water samples, J. Chromatogr. A 1216 (2009) 4361–4365.
[15] Q. Zhou, H. Bai, G. Xie, J. Xiao, Temperature-controlled ionic liquid dispersive liquid phase micro-extraction, J. Chromatogr. A 1177 (2008) 43–49.
[16] M.R.K. Zanjani, Y. Yamini, S. Shariati, J.Å. Jönsson, A new liquid-phase microextraction method based on solidification of floating organic drop,

[17] Anal. Chim. Acta 585 (2007) 286–293.
H. Liu, M. Zhang, X. Wang, Y. Zou, W. Wang, M. Ma, Y. Li, H. Wang, Extraction and determination of polybrominated diphenyl ethers in water and urine samples using solidified floating organic drop microextraction along with high performance liquid chromatography, Microchim. Acta 176 (2012) 303–309.
[18] J. Cheng, J. Xiao, Y. Zhou, Y. Xia, F. Guo, J. Li, Dispersive liquid-liquid microextraction based on solidification of floating organic droplet method for the determination of diethofencarb and pyrimethanil in aqueous samples, Microchim. Acta 172 (2011) 51–55.
[19] M.-I. Leong, S.-D. Huang, Dispersive liquid–liquid microextraction method based on solidification of floating organic drop combined with gas chromatography with electron-capture or mass spectrometry detection, J. Chromatogr. A 1211 (2008) 8–12.
[20] J. Ma, J. Zhang, X. Du, X. Lei, J. Li, Solidified floating organic drop microextraction for determination of trace amounts of zinc in water samples by flame atomic absorption spectrometry, Microchim. Acta 168 (2010) 153–159.
[21] J.A. Oviedo, L.L. Fialho, J.A. Nóbrega, Determination of molybdenum in plants by vortex-assisted emulsification solidified floating organic drop microextraction and flame atomic absorption spectrometry, Spectrochim. Acta Part B 86 (2013) 142–145.
[22] R.-J. Chung, M.-I. Leong, S.-D. Huang, Determination of nitrophenols using ultrahigh pressure liquid chromatography and a new manual shaking-enhanced, ultrasound-assisted emulsification microextraction method based on solidification of a floating organic droplet, J. Chromatogr. A 1246 (2012) 55–61.
[23] M.S. Tehrani, M.H. Givianrad, N. Mahoor, Surfactant-assisted dispersive liquid–liquid microextraction followed by high-performance liquid chromatography for determination of amphetamine and methamphetamine in urine samples, Anal. Method 4 (2012) 1357–1364.
[24] M. Mohamadi, A. Mostafavi, A novel solidified floating organic drop microextraction based on ultrasound-dispersion for separation and preconcentration of palladium in aqueous samples, Talanta 81 (2010) 309–313.
[25] M. Cruz-Vera, R. Lucena, S. Cárdenas, M. Valcárcel, One-step in-syringe ionic liquid-based dispersive liquid–liquid microextraction, J. Chromatogr. A 1216 (2009) 6459–6465.
[26] Z.-G. Shi, H.K. Lee, Dispersive liquid– liquid microextraction coupled with dispersive μ-solid-phase extraction for the fast determination of polycyclic aromatic hydrocarbons in environmental water samples, Anal. Chem. 82 (2010) 1540–1545.
[27] K.S. Tay, N.A. Rahman, M.R.B. Abas, Magnetic nanoparticle assisted dispersive liquid–liquid microextraction for the determination of 4-n-nonylphenol in water, Anal. Method 5 (2013) 2933–2938.
[28] R. Capdeville, E. Buchdunger, J. Zimmermann, A. Matter, Glivec (STI571, imatinib), a rationally developed, targeted anticancer drug, Nat. Rev. Drug Discov. 1 (2002) 493–502.
[29] B.J. Druker, M. Talpaz, D.J. Resta, B. Peng, E. Buchdunger, J.M. Ford, N.B. Lydon, H. Kantarjian, R. Capdeville, S. Ohno-Jones, Efficacy and safety of a specific inhibitor of the BCR-ABL tyrosine kinase in chronic myeloid leukemia, N. Engl. J. Med. 344 (2001) 1031–1037.
[30] R.J. Motzer, M.D. Michaelson, B.G. Redman, G.R. Hudes, G. Wilding, R.A. Figlin, M.S. Ginsberg, S.T. Kim, C.M. Baum, S.E. DePrimo, Activity of SU11248, a multitargeted inhibitor of vascular endothelial growth factor receptor and platelet-derived growth factor receptor, in patients with metastatic renal cell carcinoma, J. Clin. Oncol. 24 (2006) 16–24.
[31] M. Padmalatha, S. Kulsum, C. Rahul, D. Thimma Reddy, G. Vidyasagar, Spectrophotometric methods for the determination of erlotinib in pure and pharmaceutical dosage forms, Int. J. Pharm. Res. Dev. 3 (2011) 103–109.
[32] A. Awidi, A.O. Ayed, N. Bsoul, A. Magablah, R. Mefleh, M. Dweiri, M. Ramahi, E. Arafat, M. Bishtawi, L. Marie, Relationship of serum imatinib trough level and response in CML patients: long term follow-up, Leuk. Res. 34 (2010) 1573–1575.
[33] B. Blanchet, C. Saboureau, A.S. Benichou, B. Billemont, F. Taieb, S. Ropert, A. Dauphin, F. Goldwasser, M. Tod, Development and validation of an HPLC-UV-visible method for sunitinib quantification in human plasma, Clin. Chim. Acta 404 (2009) 134–139.
[34] C.M. Rudin, W. Liu, A. Desai, T. Karrison, X. Jiang, L. Janisch, S. Das, J. Ramirez, B. Poonkuzhali, E. Schuetz, Pharmacogenomic and pharmacokinetic determinants of erlotinib toxicity, J. Clin. Oncol. 26 (2008) 1119–1127.
[35] J.-Y. Blay, Pharmacological management of gastrointestinal stromal tumours: an update on the role of sunitinib, Ann. Oncol. (2009) mdp291.
[36] J.F. Apperley, Part I: mechanisms of resistance to imatinib in chronic myeloid leukaemia, Lancet Oncol 8 (2007) 1018–1029.
[37] R.A. Larson, B.J. Druker, F. Guilhot, S.G. O'Brien, G.J. Riviere, T. Krahnke, I. Gathmann, Y. Wang, Imatinib pharmacokinetics and its correlation with response and safety in chronic-phase chronic myeloid leukemia: a subanalysis of the IRIS study, Blood 111 (2008) 4022–4028.
[38] K. Neville, R.A. Parise, P. Thompson, A. Aleksic, M.J. Egorin, F.M. Balis, L. McGuffey, C. McCully, S.L. Berg, S.M. Blaney, Plasma and cerebrospinal fluid pharmacokinetics of imatinib after administration to nonhuman primates, Clin. Cancer Res. 10 (2008) 2525–2529.
[39] M. Baccarani, G. Saglio, J. Goldman, A. Hochhaus, B. Simonsson, F. Appelbaum, J. Apperley, F. Cervantes, J. Cortes, M. Deininger, Evolving concepts in the management of chronic myeloid leukemia: recommendations from an expert panel on behalf of the European LeukemiaNet, Blood 108 (2006) 1809–1820.

[40] J.M. Kokosa, Advances in solvent-microextraction techniques, TrAC, Trends Anal. Chem. 43 (2013) 2—13.

[41] S. Bolandnazar, A. Divsalar, H. Valizadeh, A. Khodaei, P. Zakeri-Milani, Development and application of an HPLC method for erlotinib protein binding studies, Adv. Pharm. Bull. 3 (2013) 289.

[42] M.S. Dresselhaus, G. Dresselhaus, R. Saito, A. Jorio, Raman spectroscopy of carbon nanotubes, Phys. Rep. 409 (2005) 47—99.

[43] W. Li, H. Zhang, C. Wang, Y. Zhang, L. Xu, K. Zhu, S. Xie, Raman character- ization of aligned carbon nanotubes produced by thermal decomposition of hydrocarbon vapor, Appl. Phys. Lett. 70 (1997) 2684—2686.

[44] S. Xie, W. Li, Z. Pan, B. Chang, L. Sun, Carbon nanotube arrays, Eur. Phys. J. D. 9 (1999) 85—89.

[45] M.S. Bidabadi, S. Dadfarnia, A.M.H. Shabani, Solidified floating organic drop microextraction (SFODME) for simultaneous separation/preconcentration and

[46] S. Chen, S. Zhu, D. Lu, Solidified floating organic drop microextraction for speciation of selenium and its distribution in selenium-rich tea leaves and tea infusion by electrothermal vapourisation inductively coupled plasma mass spectrometry, Food Chem. 169 (2015) 156—161.

[47] M. Alagiri, C. Muthamizhchelvan, S. Ponnusamy, Structural and magnetic properties of iron, cobalt and nickel nanoparticles, Synth. Met. 161 (2011) 1776—1780.

[48] S. Bouchet, E. Chauzit, D. Ducint, N. Castaing, M. Canal-Raffin, N. Moore, K. Titier, M. Molimard, Simultaneous determination of nine tyrosine kinase inhibitors by 96-well solid-phase extraction and ultra performance LC/MS-MS, Clin. Chim. Acta 412 (2011) 1060—1067.

determination of cobalt and nickel by graphite furnace atomic absorption spectrometry (GFAAS), J. Hazard. Mater. 166 (2009) 291—296.